International Journal of Microwave and Wireless Technologies, 2017, 9(3), 697–703.
doi:10.1017/S1759078716000519

RESEARCH PAPER

Gain enhancement of wideband circularly polarized antenna using FSS

NAGENDRA KUSHWAHA[1] AND RAJ KUMAR[2]

This paper presents a high gain, wideband circularly polarized (CP) antenna. High gain of the antenna is achieved by employing a frequency selective surface (FSS) as a reflector. The antenna is a coplanar waveguide-fed structure with a modified L-shaped radiating patch. The unit element of the FSS is formed by connecting two modified dipoles at an angle of 90°. The antenna with reflector has a measured impedance bandwidth of 74.3% (2.2–4.8 GHz) and a 3-dB axial ratio bandwidth (ARBW) of 62% (2.2–4.18 GHz). The maximum boresight gain of the proposed antenna with reflector is 7.1 dB at 3.4 GHz. The radiation patterns of the antenna with the FSS are also measured and compared with simulated patterns. The various aspects of effect of FSS on CP antenna performance are also discussed.

Keywords: Circular polarization antenna, CPW-fed antenna, FSS, High gain antenna, Reflector, Wideband antenna

Received 7 October 2015; Revised 16 March 2016; Accepted 20 March 2016; first published online 29 April 2016

I. INTRODUCTION

Recently, printed antenna technology gained much of the attention from the antenna designers due to its low profile and ease of fabrication features. Among these, circularly polarized (CP) antennas are very popular due to their merit over linearly polarized (LP) antennas in terms of Faraday rotation insensitivity, weather penetration, and no problem of the strict orientation of receiver and transmitter [1]. High data transfer rate requires a broad bandwidth and the ease of handling requires compact antennas. Coplanar waveguide (CPW)-fed slot antennas are fit into aforementioned category because these are compact, low profile, and broadband in nature. But the printed antennas suffer from a inherit disadvantage of low gain. Therefore, low-profile, high-gain printed wideband antenna with CP radiations is required to achieve the best performance out of a wireless device.

In the recent past, many efforts have been made to achieve high gain for printed CP antennas. High-gain CP antennas can be obtained either by increasing the gain of a CP antenna with the help of reflectors and superstrates [2–5] or by using a polarizer to convert LP radiations from an antenna to CP radiations [6–9]. High gain of the printed CP antenna can also be achieved by using array structure, but it requires a complex feeding structure [10, 11]. In [2], the gain of a CP antenna is increased by using frequency selective surface (FSS) as a reflector. The impedance bandwidth and the axial ratio bandwidth (ARBW) are 36.67 and 23.33%, respectively. The gain of a CPW-fed slot antenna in [3] is enhanced by a dipole-type FSS using as a reflector. The achieved ARBW is 40%. In [4], high gain of a CP antenna is achieved by using a ring-shaped FSS as a superstrate layer. The operating bandwidth of the antenna with the FSS is 2.4%. In [5], the gain of a CP antenna is enhanced by using a slot-type FSS as a superstrate layer. The operating BW is 4.73%. The above designed antennas are having narrow CP operation bandwidth.

In this paper, a high-gain, CP antenna for broadband operation is designed. The antenna is a CPW-fed slot structure excited by an L-shaped patch. An FSS is used to enhance the gain of the antenna whose unit element has two center connected modified dipoles. The FSS array is made by varying size unit elements and also made defected by removing two elements. This gives an additional degree of freedom, which helps in maintaining the ARBW. The achieved impedance bandwidth and ARBW with the FSS are 74.3 and 62%, respectively. To the best of the author's knowledge, no paper has been reported in the open literature to enhance the gain of a CP antenna with such a huge operating bandwidth. The proposed high-gain CP antenna can have applications in WLAN, WiMax, and satellite systems. CST-Microwave Studio simulation tool is used to design and analyze the antenna and FSS structure.

II. ANTENNA DESCRIPTION

For application of the FSS, the CP antenna used is the one proposed in [12] by the same authors and described below. The antenna geometry is shown in Fig. 1. A FR-4 material of thickness 1.6 mm and dielectric constant 4.4 is used as dielectric substrate. An asymmetric rectangular slot is etched out from the ground plane. This slot is excited by an L-shaped patch with a 50 Ω CPW-fed line. The patch is selected as L-shaped to generate two orthogonal modes with 90° phase difference. With this structure a very narrow ARBW is achieved. To

[1]Department of Electronics Engineering, DIAT (DU), Pune-411025, India
[2]Department of Armament Electronics, ARDE, Pune-411021, India
Corresponding author:
R. Kumar
Email: dr.rajkumarkumar@yahoo.com

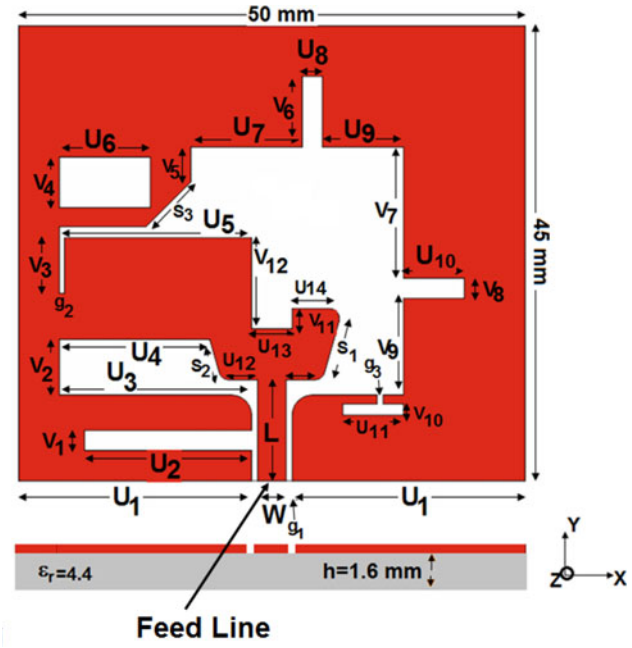

Fig. 1. Geometry of the CP antenna.

increase the ARBW, the surface current distributions and electric field distribution are studied on either side of the achieved CP operation frequency. By judicially etching out two horizontal slots the ARBW is improved. Further to improve the ARBW at the lower frequency side one end of the L-shaped patch is connected to the ground. By this the ARBW improves at the lower frequencies. Also an inverted T-shaped slot is etched out from the ground plane to get wider ARBW. The detail description of the antenna design is discussed in [12]. The optimized dimensions of the antenna are given in Table 1.

Table 1. Optimized dimensions of the antenna in mm.

Parameter	U_1	U_2	U_3	U_4	U_5	U_6	U_7
Value	23	16.7	19	14.5	18.5	9	11
Parameter	U_8	U_9	U_{10}	U_{11}	U_{12}	U_{13}	U_{14}
Value	2	8	6	6	3.5	4	4
Parameter	V_1	V_2	V_3	V_4	V_5	V_6	V_7
Value	2	5.5	5.5	5	3.5	7	13
Parameter	V_8	V_9	V_{10}	V_{11}	V_{12}	S_1	S_2
Value	2	9.5	1.1	9	2	4.5	6.3
Parameter	S_3	L	i	g_1	g_2	g_3	
Value	5.2	10	2.8	0.6	0.5	0.8	

To understand the etching of the slots in the ground plane, current distributions for two cases are given in Fig. 2 at 4 GHz. In the first case there is no slot in the ground plane, while in the second case two slots have been etched in the ground plane. From the figure it can be seen that when there is no slot in the ground plane, the difference between amplitudes of horizontal current and vertical current is large. And after etching the two slots in the ground plane, the difference between horizontal current and vertical current amplitude is small. This is due to a decrease in the vertical current in the ground plane after the etching of the slot. Therefore cutting slots in the ground plane nearly equalizes the both orthogonal modes current amplitudes.

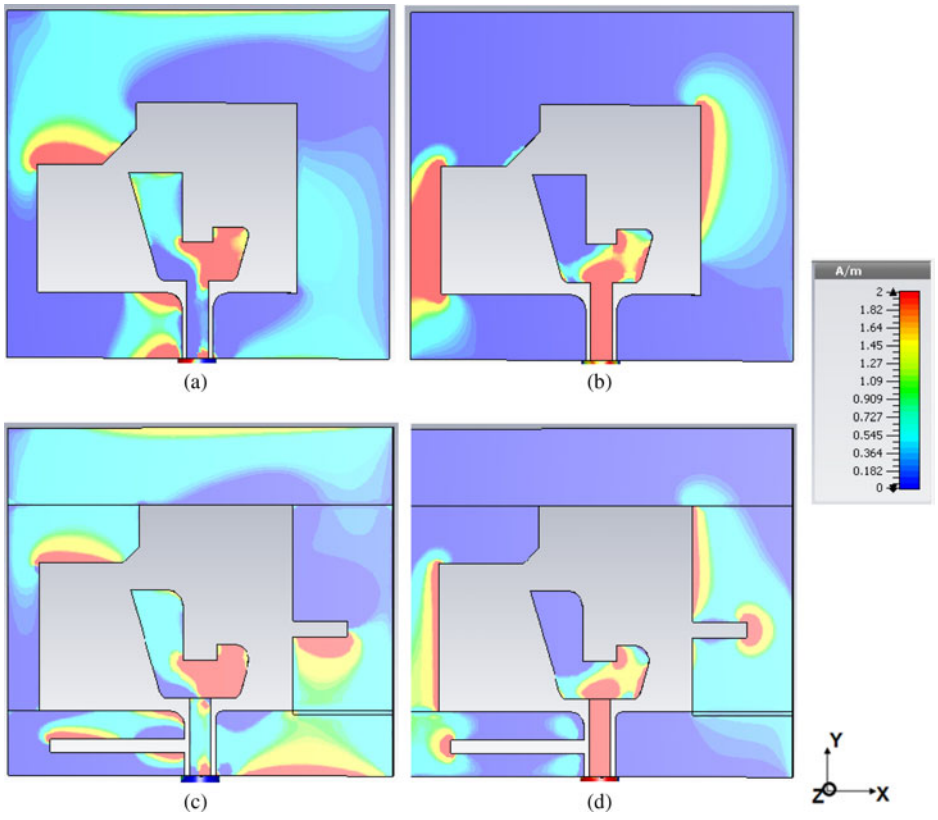

Fig. 2. Current distribution at 4 GHz. (a) Horizontal current distribution without slot; (b) vertical current distribution without slot; (c) horizontal current distribution with slot; (d) vertical current distribution with slot.

https://doi.org/10.1017/S1759078716000519 Published online by Cambridge University Press

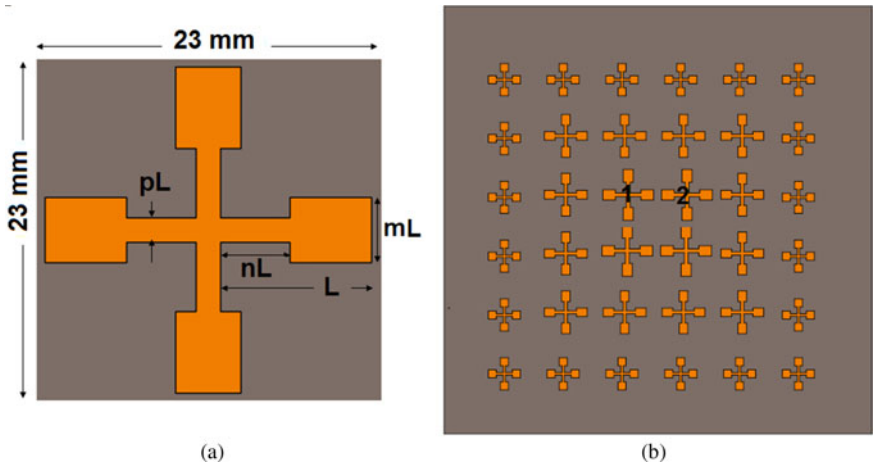

Fig. 3. Proposed FSS structure: (a) unit element; (b) FSS array.

III. FSS UNIT ELEMENT AND ARRAY DESIGN

The geometry of the unit element of the FSS is shown in Fig. 3(a). The FSS is designed on the FR-4 substrate of thickness 1.6 mm and dielectric constant 4.4 mm. The unit element is designed using two modified symmetric dipoles connected at the center at an angle 90°. The unit element structure is chosen such that it can reflect the two orthogonal waves with nearly same characteristics. The dipoles are of steps structure such that the center of the dipole is narrower while both the sides of the dipole are wider. The step design is chosen to increase the electrical length of the FSS element. The dimension of a unit element is selected as 23×23 mm^2. The total length of the dipole is $2L$. The length of the narrow section is $2nL$, while the wider section is $2L(1-n)$ mm long. The width of the narrow section is pL, while wider is mL. The length and width of the sections are selected in terms of total length of the dipole, so that by only changing the length, the structure is easily optimized.

The FSS array is designed using variable size unit elements. The size of the elements is varied successively such that the elements located at the center of the array have larger size, while the elements at outer has smallest size. The sizes of the patches are chosen in the aforementioned manner to compensate the phase mismatch due to difference in the path length for the center elements and the elements at the edge of the FSS array. As the path length between antenna and the center of the array is smaller as comparison with the path length between antenna and elements at the edge of the array. Therefore, to compensate the phase difference due to difference in path length the center elements are chosen bigger, while elements at the edges are smaller. The FSS array is shown in Fig. 3(b). As discussed earlier, the dimensions of the modified dipole depend on its length. Therefore, the length of the dipole is varied and the other dimensions are automatically changed according to the value of m, n, and p. Initially, for the innermost elements the length L is selected as $L_1 = 9.5$ mm and the values of m, n, and p are selected as 0.2, 0.5, and 0.075, respectively. Then the length is changed to L_2, L_3,

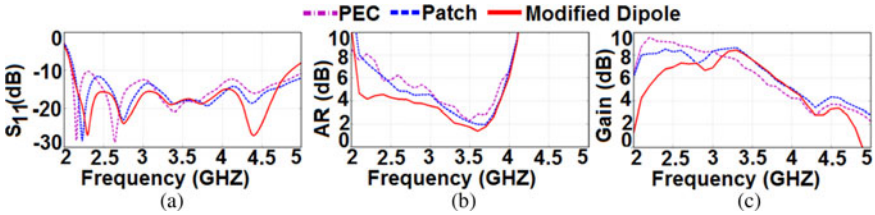

Fig. 4. Comparison of different reflector effect on antenna characteristics: (a) S_{11}; (b) AR; (c) boresight gain.

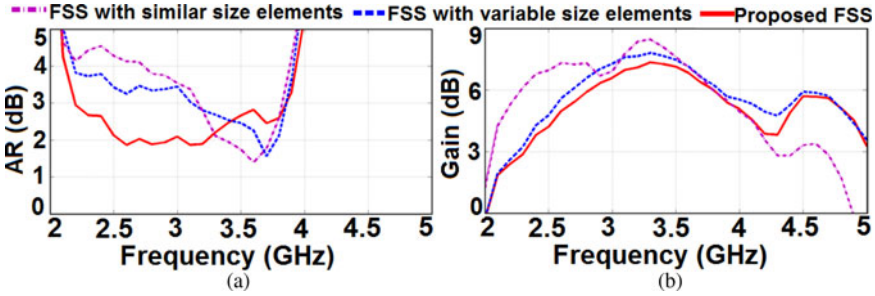

Fig. 5. Comparison of characteristics of antenna with conventional FSS structure and defected FSS structure: (a) AR; (b) boresight gain.

https://doi.org/10.1017/S1759078716000519 Published online by Cambridge University Press

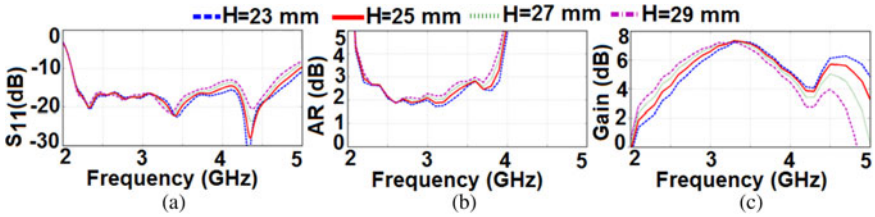

Fig. 6. Comparison of antenna with FSS characteristics for different values of distance H between the FSS and antenna: (a) S_{11}; (b) AR; (c) boresight gain.

Table 2. Optimized dimensions of the antenna after application of FSS in mm.

Parameter	U_2	U_7	U_8	U_9	U_{10}	V_6
Dimension	19.1	17	3	1	4	7.5
Parameter	V_7	V_8	V_9	V_{12}	W	g_2
Dimension	13.5	4	7.5	0.5	2.6	2.2

and L_4 for the successive elements in the array. The values of the lengths L_2, L_3, and L_4 are optimized after application of FSS on antenna structure and it is given in Section IV. The overall size of the array is 150×150 mm^2.

For better understanding, the selection of unit element shape, variation of the size of the elements in the array and finally making the array defective is discussed. At the first, the characteristics of the antenna after applying three different types of reflectors are discussed. The first reflector is selected as a perfect electric conductor (PEC) reflector, the second reflector is an FSS reflector made from square patches and the third is also an FSS reflector made by the proposed unit element (modified crossed dipole). The side length of the patch is chosen same as the length of the modified dipole. Both the FSS arrays are made with the similar size and same no. of elements. Figure 4 shows a comparison of the antenna characteristics after applying the earlier mentioned three reflectors. Figure 4(a) shows the reflection coefficients (S_{11}) of the three cases. It can be seen from the figure that the reflector with proposed modified element has better S_{11} than the other two. This is due to out of phase multiple reflections of waves by the PEC reflector and patch reflector, which is minimized in the case of the reflector with the proposed element. Similarly, from Fig. 4(b) it can be seen that antenna with the modified dipole reflector has AR values less than antenna with the other reflectors. Figure 4(c) shows the bore sight gain comparison of the antenna with the three reflectors. From the figure, it can be seen that the antenna with proposed element reflector has lesser gain as compared to antenna with the other two reflectors especially at the lower frequencies. But the other two reflectors have poor impedance matching and greater AR values. The aim of this work is to enhance the gain of the antenna, while maintaining its impedance bandwidth and AR characteristics as earlier. Therefore, keeping in the view of impedance bandwidth and ARBW, the proposed shape is a better candidate to increase the gain of a CP antenna.

To further understand the proposed FSS array structure, a comparison of antenna characteristics after applying the three different FSS arrays with the proposed element shape as unit element is discussed. The first array is made of similar size elements; the second is made by varying the size of the elements successively as discussed above and third array is made by etching two elements selectively making the FSS defected. The comparisons of AR and boresight gain are shown in Fig. 5. The comparison of the S_{11} of the three cases is not shown because in all the three cases the S_{11} remains nearly the same. From the figure, it can be seen that using the FSS array with similar size elements increases the gain, but it deteriorates the AR at the lower frequencies. When the FSS array is made of variable size elements the AR is improved in comparison with similar size element FSS array at the cost of reduction in the gain at the lower frequencies. Finally, the FSS array is made defected by etching out two elements, which further reduces the AR and increases the ARBW significantly.

IV. APPLICATION OF FSS ON ANTENNA

A) Design considerations

The FSS is used as a reflector to increase the gain of the antenna. The distance between the FSS and antenna "H" is selected as $\lambda/4$ at the center frequency of operation. Further, by simulation the distance between the antenna and the FSS is optimized and found to be 25 mm. A comparison of the antenna characteristics after applying the FSS for different values of H is shown in Fig. 6 for the proposed shape of the unit element. Figure 6(a) shows the reflection coefficient,

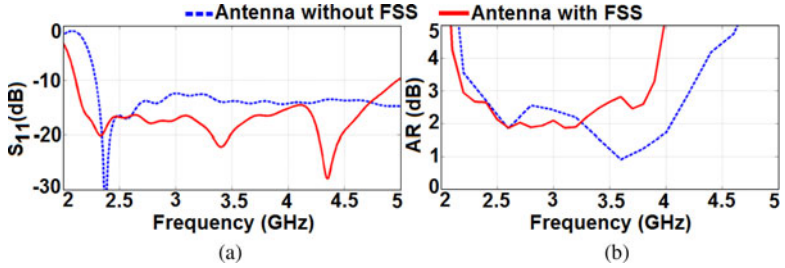

Fig. 7. Comparison of antenna characteristics with and without the FSS: (a) S_{11}; (b) AR.

https://doi.org/10.1017/S1759078716000519 Published online by Cambridge University Press

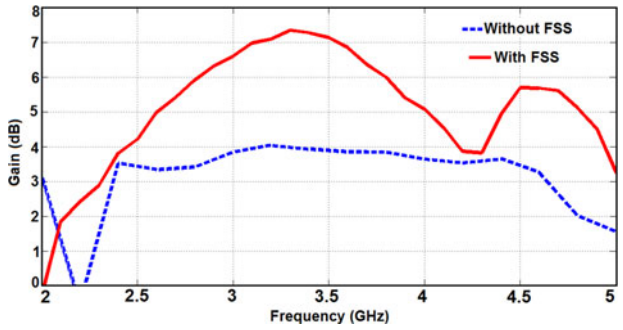

Fig. 8. Comparison of simulated boresight gain of antenna with and without FSS.

while Fig. 6(b) shows the AR comparison. From the figure, it can be seen that H values have a very less effect on the lower frequency side. While at the higher frequency side, it has greater effect on the reflection coefficient and AR both such that with an increase in the value of H both S_{11} and AR deteriorate. Figure 6(c) shows the boresight gain comparison. From the figure, it can be seen that with increase in the value of H the boresight gain at the lower frequencies improves but deteriorates at the higher frequency. So there is a need of optimizing the value of H for higher gain throughout the operation band keeping in the view S_{11} and AR. The value of H is optimized and found to be 25 mm.

After application of FSS at 25 mm below the antenna, it is found from simulation that CP operation of the antenna is deteriorated due to different phase reflections by different elements in the FSS array which changes the electric field and surface current of the antenna. To maintain the ARBW, the FSS parameters and the antenna parameters are optimized keeping the view of ARBW. From simulation, it is found that at the lower frequencies the CP deterioration problem is still unsolved. To solve this problem, the current distributions and the electric field distribution on the FSS at the lower frequencies are investigated. On investigation, it is found that the two center elements of the FSS directly under the antenna (marked 1 and 2 in Fig. 3) have maximum reflection of fields at the lower frequencies. Therefore, these two elements are completely etched out from the FSS making FSS array a defected FSS array to achieve the wider ARBW. The disadvantage of the making the FSS defected is the slight reduction in the gain when compared with FSS array without defect. The optimized values of L_1, L_2, L_3, and L_4 are 9.5, 8, 6, and 4 mm, respectively. The optimized values of the antenna parameters which are changed after application of the FSS are shown in Table 2. All the other parameters which are not given in Table 2 are kept at their initial optimized values given in Table 1.

B. Comparison of antenna characteristics with and without FSS

The proposed FSS is used to enhance the gain of the antenna keeping in view of maintaining the impedance bandwidth and ARBW. Figure 7 shows a comparison of the reflection coefficients (S_{11}) and AR of the antenna with and without application of the FSS. From the figure, it can be seen that there is a slight decrease in the impedance bandwidth of the antenna and the impedance bandwidth also shifts toward the lower frequency side after application of the FSS. Similarly, in case of the ARBW performance, the ARBW slightly decreases and also shifts toward the lower frequency side after application of the proposed FSS. Therefore, after application of the FSS, the antenna impedance bandwidth and ARBW is nearly maintained to its original values. Figure 8 shows a comparison of the boresight gain of antenna with and without FSS. From the figure, it can be seen that there is a maximum 3 dB enhancement in the boresight gain of the antenna after application of the FSS in the CP operation band. The decrease in the boresight gain at 4.3 GHz is due to the tilting of the main lobe off the boresight direction. Figure 9 shows a simulated comparison of the radiation patterns of antenna with and without FSS. From the figure, it can be seen that after application of the FSS, the radiation at the boresight increases and the beamwidth of the antenna also becomes narrow as compares with antenna without FSS. The side lobes of the antenna after application of the FSS are also suppressed. Moreover, the back lobes of the antenna are also reduced in both the planes.

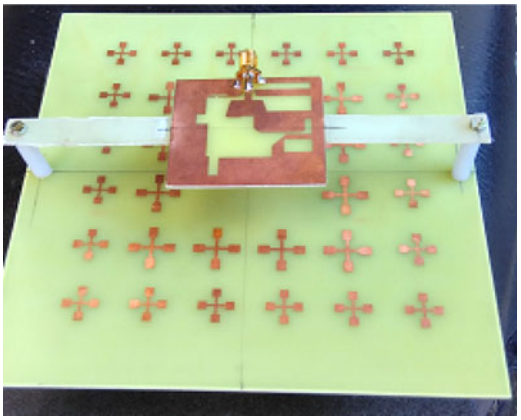

Fig. 10. Fabricated prototype of antenna along with FSS.

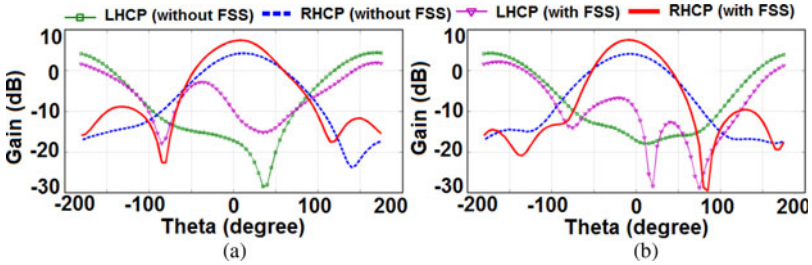

Fig. 9. Comparison of simulated radiation patterns of antenna with and without FSS: (a) Y–Z plane; (b) X–Z plane.

https://doi.org/10.1017/S1759078716000519 Published online by Cambridge University Press

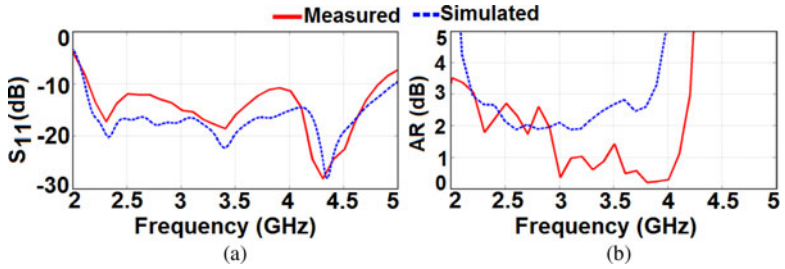

Fig. 11. Simulated and measured comparison of antenna with proposed FSS: (a) S_{11}; (b) AR.

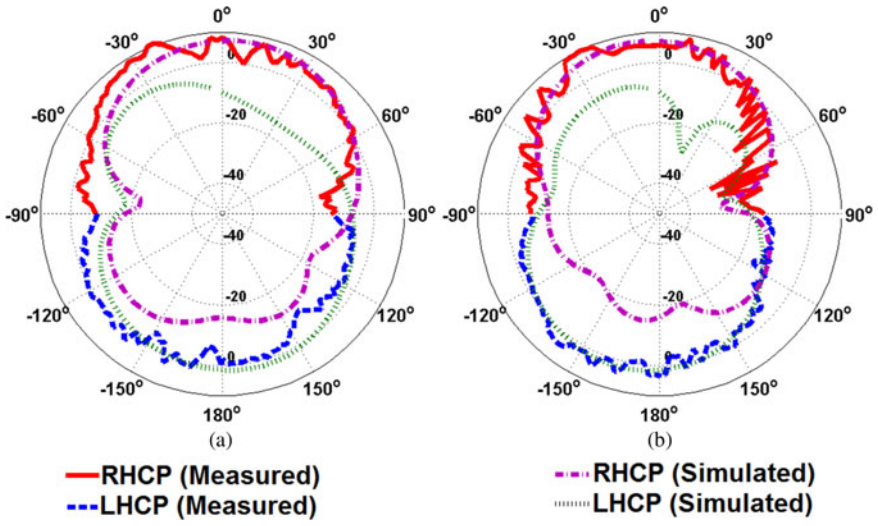

Fig. 12. Simulated and measured comparison of CP radiation patterns of the antenna with proposed FSS: (a) *Y*–*Z* plane; (b) *X*–*Z* plane.

C. Measured and simulated results

The antenna and the FSS are fabricated with the optimized dimensions. The antenna is placed at a distance of 25 mm above the proposed FSS as shown in Fig. 10. The reflection coefficient of the proposed antenna is measured using an R&S vector network analyzer ZVA40. A comparison of the simulated and measured reflection coefficient of the antenna with the proposed FSS is shown in Fig. 11(a). From the figure, it can be seen that the measured and simulated results are in good agreements. The measured impedance bandwidth of the antenna with the proposed FSS is 2.6 GHz (2.2–4.8 GHz). The radiation patterns of the antenna with the FSS are measured in an in-house anechoic chamber with conjugation of a vector network analyzer ZVA40. Procedure given in [13] is followed to calculate the CP radiation patterns and AR. The measured and simulated AR of the antenna with the proposed FSS is compared and shown in Fig. 11(b). It can also be noticed that the measured 3 dB ARBW is greater than the simulated; this is due to the increased cross-polarization of the LP reference antenna. The measured ARBW is 2 GHz (2.2–4.2 GHz). The measured and simulated CP radiation patterns are compared at 3.4 GHz in both the planes and shown in Fig. 12. From the figure, it can be seen that the measured and simulated radiation patterns are in good agreement. It can also be noticed that, at the boresight the cross-polarization level is $<$10 dB. The boresight gain of the antenna with the FSS is measured in the operating band of the antenna and compared with the simulated gain and it is shown in Fig. 13. From the figure, it can be seen that the measured and simulated results are in good agreement. Also, the maximum boresight gain is 7.1 dB at 3.4 GHz in the operating CP band.

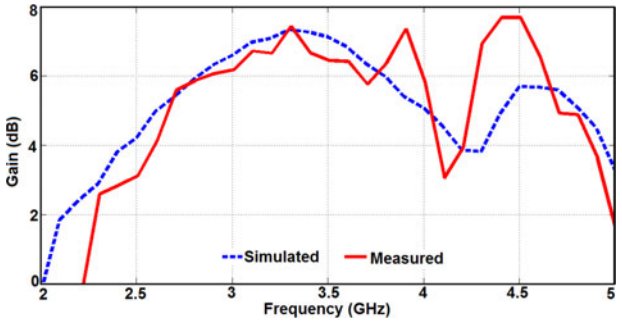

Fig. 13. Simulated and measured boresight gain comparison of antenna with the proposed FSS.

V. CONCLUSIONS

A high-gain, wideband antenna for CP operation is designed and experimentally validated. The high gain of the antenna is achieved by using an FSS as a reflector for a CPW-fed slot antenna with CP radiation patterns. To maintain the CP radiation patterns after application of the FSS, the FSS array is

https://doi.org/10.1017/S1759078716000519 Published online by Cambridge University Press

made defected by selectively etching out two elements. The antenna with the FSS has a measured impedance bandwidth and ARBW of 74.28 and 62%, respectively. The boresight gain of the antenna is significantly enhanced in the operating CP band after application of the FSS. The proposed antenna with FSS has applications in WLAN, WIMax, and satellite systems.

ACKNOWLEDGEMENT

The authors acknowledge the Vice Chancellor of DIAT (DU) for financial help in the form for fellowship.

REFERENCES

[1] Gao, S.; Luo, Q.; Zhu, F.: Circularly Polarized Antennas, Wiley, UK, 2014.

[2] Agarwal, K.; Alphones, A.: Unidirectional wideband circularly polarised aperture antennas backed with artificial magnetic conductor reflectors. IET Microw. Antennas Propag., **7** (5) (2013), 338–346.

[3] Krishna, R.R.; Kumar, R.; Kushwaha, N.: A circularly polarized slot antenna for high gain applications. AEU-Int. J. Electron. Commun., **68** (11) (2014), 1119–1128.

[4] Lee, D.H.; Lee, Y.J.; Yeo, J.; Mittra, R.; Park, W.S.: Directivity enhancement of circular polarized patch antenna using ring-shaped frequency selective surface superstrate. Microw. Opt. Technol. Lett., **49** (1) (2007), 199–201.

[5] Kushwaha, N.; Kumar, R.: Design of slotted ground hexagonal microstrip patch antenna and gain improvement with FSS screen. Progr. Electromagn. Res. B, **51** (2013), 177–199.

[6] Euler, M.; Fusco, V.; Dickie, R.; Cahill, R.; Verheggen, J.: Sub-mm wet etched linear to circular polarization FSS based polarization converters. IEEE Trans. Antennas Propag., **59** (8) (2011), 3103–3136.

[7] Ma, X.; Huang, C.; Pu, M.; Hu, C.; Feng, Q.; Luo, X.: Single-layer circular polarizer using metamaterial and its application in antenna. Microw. Opt. Technol. Lett., **54** (7) (2012), 1770–1774.

[8] Sohail, I.; Ranga, Y.; Esselle, K.P.; Hay, S.G.: A linear to circular polarization converter based on Jerusalem-cross frequency selective surface, in 2013 7th European Conf. on Antennas and Propagation (EuCAP), Gothenburg, 8 April 2013, 2141–2143.

[9] Orr, R.; Goussetis, G.; Fusco, V.: Design method for circularly polarized Fabry–Perot cavity antennas. IEEE Trans. Antennas Propag., **62** (1) (2014), 19–26.

[10] Chen, Z.N.; Esselle, K.P.: Wideband circularly polarized microstrip antenna array using a new single feed network. Microw. Opt. Technol. Lett., **50** (7) (2008), 1784–1789.

[11] Chan, K.K.; Tan, A.E.; Rambabu, K.: Decade bandwidth circularly polarized antenna array. IEEE Trans. Antennas Propag., **61** (11) (2013), 5435–5443.

[12] Kushwaha, N.; Kumar, R.; Ram Krishna, R.V.: Design and analysis of CPW-fed wideband circularly polarized antenna for modern communication systems. J. Electromagn. Waves Appl., **29** (11) (2015), 1397–1409.

[13] Toh, B.Y.; Cahill, R.; Fusco, V.F.: Understanding and measuring circular polarization. IEEE Trans. Educ., **46** (3) (2003), 313–318.

Nagendra Kushwaha received his B.Tech. degree in Electronics and Communication from Galgotia's College of Engineering and Technology Greater Noida, UP, India in 2010. He received his M.Tech. degree in Microwave Electronics from the University of Delhi South Campus, New Delhi, India in 2012. Currently, he is with Defence Institute of Advanced Technology, Pune, India and he is working toward his Ph.D. degree. He is a student member of IEEE. His current research includes microwave and millimeter-wave circuits, especially frequency selective surface (FSS), electromagnetic band gap (EBG), metamaterials, and printed antennas.

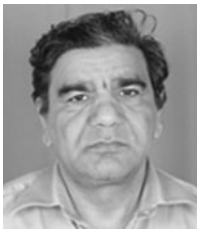

Raj Kumar was born on 14 May 1963 in Muzaffarnagar, UP, India. He completed his M.Sc. degree in Electronics in 1987 from the University of Meerut, Meerut, India. He was awarded the M.Tech. and Ph.D. degrees in Microwaves in 1992 and 1997, respectively, from the University of Delhi South Campus, New Delhi, India. He worked at CEERI, Pilani from 1993 to 1994 as a Research Associate. From May 1997 to June 1998, he worked as an Assistant Professor at Vellore College of Engineering (VIT), Vellore. He worked in DLRL (DRDO), Hyderabad as a Scientist from June 1998 to August 2002 and later on joined DIAT, Pune and worked in the Department of Electronics Engineering till September 2012. Since October 2012, he has been working in ARDE, Pune. His field of interest is microwave components, antennas, electromagnetic band-gap, frequency selective surface, filters, multiplexers, power dividers, couplers, numerical techniques, and ANN for microwave circuits and antennas.

https://doi.org/10.1017/S1759078716000519 Published online by Cambridge University Press